A Luminescent Dinuclear Eu^{III}/Tb^{III} Complex with LMCT Band for Single-molecular Thermosensor

Kei Yanagisawa,[b] Yuichi Kitagawa,[a] Takayuki Nakanishi,[a] Tomohiro Seki,[a] Koji Fushimi,[a] Hajime Ito,[a] and Yasuchika Hasegawa*[a]

Abstract: Temperature-dependent luminescence of a dinuclear Eu^{III}/Tb^{III} complex with a seven-coordinate structure is demonstrated. The dinuclear complex is composed of two lanthanide ions, six tetramethylheptanedionate ligands, and a bidentate phosphine oxide linker ligand. The dinuclear structure of the complex was characterized by single-crystal X-ray analysis. Intrinsic 4*f*-4*f* emission quantum yields of the dinuclear Eu^{III} and Tb^{III} complexes were found to be 66% and 61%, respectively. The luminescence color of the dinuclear Eu^{III}/Tb^{III} complex changed unusually from red to green with increasing temperature. The thermosensing range using the ratio of luminescence intensity (A_{Eu}/A_{Tb}) was 100-450 K. The temperature-dependent luminescence is caused by the presence of a ligand-to-metal charge transfer state.

Introduction

Temperature-sensitive luminescent nano compounds have potential applications as thermometric materials in the field of microelectronics and microfluidics due to their fast responses, noninvasive operations, and nano-scale high resolutions.[1] Various luminescent nano materials including boron-based organic molecules,[2] gold nanoclusters,[3] semiconductor quantum-dots,[4] and lanthanide-doped upconverting nanoparticles[5] have been reported as thermosensing materials. In these materials, photophysical parameters such as emission lifetime, emission wavelength, and emission intensity have been utilized for thermosensing performance. Recently, thermometric methods using the ratio of luminescent intensities from multiple emission centers have been developed for accurate thermosensing measurements.[6] Dual-emissive thermometry is not affected by excitation intensity of the light source, concentration of the emitter, and/or sensitivity of the optical detector. In terms of accurate measurements, narrow full-width at half-maximum (fwhm) of each emission band is useful for calculation of the ratio of luminescence intensity.

[a] Y. Kitagawa, T. Nakanishi, T. Seki, K. Fushimi, H. Ito, Y. Hasegawa
Faculty of Engineering
Hokkaido University
Kita-13 Jo, Nishi-8 Chome, Kita-ku, Sapporo, Hokkaido, 060-8628 (Japan)
E-mail: hasegaway@eng.hokudai.ac.jp
[b] K. Yanagisawa
Graduate School of Chemical Sciences and Engineering
Hokkaido University
Kita-13 Jo, Nishi-8 Chome, Kita-ku, Sapporo, Hokkaido 060-8628 (Japan)

Supporting information for this article is given via a link at the end of the document.

Thermosensing materials constructed from lanthanide complexes have been increasingly studied due to the narrow fwhm of emission bands.[7] The narrow bandwidths originate from 4*f*-4*f* transitions because of little change in the electronic structures between ground and excited states. Since the emission wavelength of 4*f*-4*f* transitions is independent of the surrounding environment, the emission color can be controlled by selection of lanthanide ions (Eu^{III}: red, Tb^{III}: green, and Yb^{III}: near-infrared). Carlos pioneered luminescence thermometry based on dual-emission of Eu^{III}/Tb^{III} hybridized organosilica on Fe_2O_3 nanoparticles (sensing range: 10-350 K).[6] Qian demonstrated the first example of a luminescent metal organic framework (MOF) including Eu^{III} and Tb^{III} for a ratiometric thermometer (sensing range: 10-300 K).[8] Our research group also reported a luminescent coordination polymer named 'chameleon luminophore' containing Eu^{III} and Tb^{III} with high thermostability (sensing range: 200-500 K).[9]

Temperature-dependent luminescence of Eu^{III}/Tb^{III} complexes are attributed to 1) energy gap dependence: back energy transfer from the $^5D_4$ configuration of Tb^{III} to the excited triplet state (T_1) of organic ligands[10] and/or 2) activation energy dependence: phonon-assisted energy transfer from Tb^{III} to Eu^{III}.[11] These dependences concerned with thermo-sensitivity induce typical emission color change (green to red) with increasing temperature. Here, we have attempted to utilize ligand-to-metal charge transfer (LMCT) transition of lanthanide complexes for effective thermosensing properties. The LMCT band is observed in Eu^{III}-tetramethylheptanedionate (tmh) complexes and promotes non-radiative relaxation.[12-14] The quenching mechanism by LMCT band has been also proposed theoretically.[15] The fast relaxation process through the LMCT band is expected to produce unprecedented thermo-sensitive luminescence properties.

In this study, we synthesized new seven-coordinate dinuclear complexes composed of two lanthanide ions, six tmh ligands, and a 4,4'-bis(diphenylphosphoryl)biphenyl (dpbp) ligand {[$Eu_2(tmh)_6$dpbp], [$Tb_2(tmh)_6$dpbp], and [$EuTb(tmh)_6$dpbp] in Figure 1a} for introduction of a LMCT band into dual-emissive thermometry. The dinuclear structures were determined by single-crystal X-ray diffraction analysis. Photophysical properties of the dinuclear complexes were evaluated using absorption, emission, and excitation spectra. Radiative and non-radiative rate constants (k_r and k_{nr}) were calculated using emission lifetimes (τ_{obs}) and 4*f*-4*f* emission quantum yields (Φ_{ff}). Unexpectedly, the dinuclear Eu^{III}/Tb^{III} complex, [$EuTb(tmh)_6$dpbp], showed gradual emission color change from red to green with increasing temperature (Figure 1b). The thermosensing range using the ratio of luminescence intensity (A_{Eu}/A_{Tb}) was found to be 100-450 K. We also found that the thermosensing ability is based on the presence of a LMCT band,

Table 1. Crystallographic data of [EuTb(tmh)$_6$dpbp], [Eu$_2$(tmh)$_6$dpbp], [Tb$_2$(tmh)$_6$dpbp], and [Gd$_2$(tmh)$_6$dpbp].

	[EuTb(tmh)$_6$dpbp]	[Eu$_2$(tmh)$_6$dpbp]	[Tb$_2$(tmh)$_6$dpbp]	[Gd$_2$(tmh)$_6$dpbp]
chemical formula	$C_{102}H_{142}EuO_{14}P_2Tb$	$C_{102}H_{142}Eu_2O_{14}P_2$	$C_{102}H_{142}O_{14}P_2$ Tb_2	$C_{102}H_{142}Gd_2O_{14}P_2$
formula weight	1964.97	1958.01	1971.93	1968.61
crystal system	monoclinic	monoclinic	monoclinic	monoclinic
space group	*P* 2$_1$/*n*	*P* 2$_1$/*n*	*P* 2$_1$/*n*	*P* 2$_1$/*n*
a [Å]	22.2487 (8)	22.2843 (5)	22.2894 (6)	22.2685 (5)
b [Å]	12.9155 (5)	12.9376 (4)	12.9348 (3)	12.9311 (3)
c [Å]	35.9989 (14)	36.0342 (7)	36.0983 (7)	36.0097 (7)
β [º]	95.331 (7)	95.2528 (7)	95.372 (1)	95.402 (1)
V [Å^3]	10299.6 (7)	10345.2 (4)	10361.7 (4)	10323.2 (4)
Z	4	4	4	4
d_{calcd} [g cm^{-1}]	1.267	1.257	1.264	1.267
T [K]	123	123	123	123
R[a]	0.0641	0.0507	0.0372	0.0563
wR[b]	0.1396	0.1264	0.0888	0.1297

[a] $R = \Sigma||F_0|—|F_c|| / \Sigma|F_0|$. [b] $wR = [(\Sigma w(|F_0|—|F_c|)^2 / \Sigma wF_0^2)]^{1/2}$.

by Arrhenius analysis of the emission lifetime. The characteristic temperature-dependent luminescence of the dinuclear Eu^{III}/Tb^{III} complex including a LMCT band is demonstrated as a single-molecular thermosensor.

Results and Discussion

Structural and photophysical analyses

Dinuclear lanthanide complexes {[Eu$_2$(tmh)$_6$dpbp], [Tb$_2$(tmh)$_6$dpbp], and [EuTb(tmh)$_6$dpbp]} were synthesized by the reaction of a precursor complex [Ln(tmh)$_3$(MeOH)$_2$] (Ln = Eu^{III} and/or Tb^{III}) with dpbp in methanol under reflux for 6 h. A dinuclear Gd^{III} complex, [Gd$_2$(tmh)$_6$dpbp], was also prepared for estimation of the energy level of T_1 of the organic ligands. Single crystals of all of the dinuclear complexes were obtained from recrystallization from methanol at room temperature. The crystallographic data for [EuTb(tmh)$_6$dpbp], [Eu$_2$(tmh)$_6$dpbp], [Tb$_2$(tmh)$_6$dpbp], and [Gd$_2$(tmh)$_6$dpbp] is shown in Table 1. The lattice constants in a monoclinic system of [EuTb(tmh)$_6$dpbp] were similar to those of [Eu$_2$(tmh)$_6$dpbp], [Gd$_2$(tmh)$_6$dpbp], and [Tb$_2$(tmh)$_6$dpbp]. The ORTEP view of [Eu$_2$(tmh)$_6$dpbp] is shown in Figure 2. In this dinuclear structure, two units of [Eu(tmh)$_3$] are connected with a dpbp ligand. Average bond lengths between Eu and O atoms in tmh and dpbp ligands were 2.33 and 2.35 Å, respectively. These relatively short distances are similar to those of previously reported seven-coordinate Eu^{III} complexes.[14,16] We carried out shape-factor calculation based on the crystal structure to estimate the coordination geometry around Eu^{III}. The geometrical structure of [Eu$_2$(tmh)$_6$dpbp] was categorized as a distorted monocapped-octahedron (see supporting information, Tables S1 and S2).[17,18] TG-DTA analysis revealed that the decomposition temperature of [Eu$_2$(tmh)$_6$dpbp] was 495 K (Figure S1).

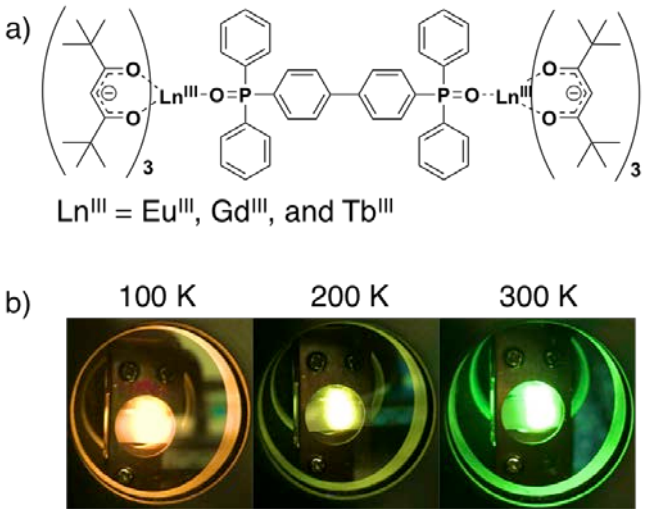

Figure 1. a) Chemical structure of [Ln$_2$(tmh)$_6$dpbp] and b) the luminescence color at 100-300K.

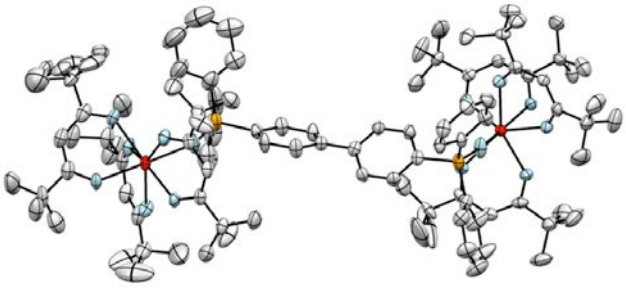

Figure 2. ORTEP drawing of $[Eu_2(tmh)_6dpbp]$. Hydrogen atoms are omitted for clarity. Thermal ellipsoids are shown at the 50% probability.

Figure 3a shows absorption, excitation, and emission spectra of $[Eu_2(tmh)_6dpbp]$ in the solid state at room temperature. The absorption band at around 320 nm is attributed to singlet π-π^* and/or σ-π^* transitions of the tmh ligands.[14] Additionally, the shoulder band at around 370 nm is based on LMCT ($tmh \rightarrow Eu^{III}$) transition. The LMCT band in the Eu^{III} complex was experimentally confirmed by comparison with absorption spectrum of $[Gd_2(tmh)_6dpbp]$ (Figure S2).[19] In contrast, we cannot observe an effective excitation band in the UV region, due to inefficient photosensitized energy transfer from the ligands to Eu^{III}. The excitation spectrum shows distinguishable 4*f*-4*f* absorption bands in the visible region [$^5L_6$ and ^5D_J (J = 0-3)$\leftarrow ^7F_J$ (J = 0,1)].[20] In the case of absorption spectrum for $[Tb_2(tmh)_6dpbp]$ (Figure 3b), π-π^* and/or σ-π^* bands without a LMCT band are observed in the UV region. The excitation spectrum clearly shows intense bands based on photosensitized luminescence at around 330 nm. The shoulder band at approximately 380 nm is 4*f*-4*f* transition of Tb^{III} ($^5D_3 \leftarrow ^7F_6$).[21]

The emission spectra of $[Eu_2(tmh)_6dpbp]$ and $[Tb_2(tmh)_6dpbp]$ exhibit typical 4*f*-4*f* transitions [Eu^{III}: $^5D_0 \rightarrow ^7F_J$ (J = 0-4) and Tb^{III}: $^5D_4 \rightarrow ^7F_J$ (J = 6-0)]. The characteristic spectral shapes with wide Stark splitting of $[Eu_2(tmh)_6dpbp]$ (Figure S3a) and $[Tb_2(tmh)_6dpbp]$ (Figure S3b) are similar to those of previously reported Eu^{III} and Tb^{III} complexes with low-symmetrical seven-coordinate structures.[14, 22]

The τ_{obs} values of $[Eu_2(tmh)_6dpbp]$, $[Tb_2(tmh)_6dpbp]$, and $[EuTb(tmh)_6dpbp]$ were obtained from time-resolved luminescence decay profiles (Figure S4 and S5). The emission profiles for $[EuTb(tmh)_6dpbp]$ was single-exponential decay curves. Therefore, the luminescence properties for $[EuTb(tmh)_6dpbp]$ is expected to be mainly due to heterometallic dinuclear complex. The τ_{obs} for $[EuTb(tmh)_6dpbp]$ monitored at 548 nm ($^5D_4 \rightarrow ^7F_5$) and 611 nm ($^5D_0 \rightarrow ^7F_2$) were 0.90 ms and 0.76 ms, respectively. The values were different from those for homometallic complexes. The decrease in lifetime of Tb^{III} emission is attributed to energy transfer to Eu^{III}. The increase in that of Eu^{III} emission is assumed to be due to suppression of concentration quenching between Eu^{III} ions.

Total emission quantum yields (Φ_{tot}) excited at 330 nm were directly measured with an integrating-sphere unit. The values of Φ_{ff} (excited at 464 nm for Eu^{III} and excited at 483 nm for Tb^{III}) were also estimated by the same method as that for Φ_{tot}. The magnitudes of k_r and k_{nr} were calculated using τ_{obs} and Φ_{ff}. These photophysical properties of $[Eu_2(tmh)_6dpbp]$, $[Tb_2(tmh)_6dpbp]$, and $[EuTb(tmh)_6dpbp]$ are summarized in Table 2. The value of Φ_{tot} for $[Eu_2(tmh)_6dpbp]$ was 0.5%, which is due to thermal relaxation from the LMCT state before photosensitized energy transfer from T_1 to Eu^{III}.[12-15] On the other hand, $[Tb_2(tmh)_6dpbp]$ exhibited relatively high Φ_{tot} (56%). The high value is comparable to previously reported emission quantum yields of the Tb^{III} complexes with efficient luminescence.[23-25] The large energy gap between T_1 and $^5D_4$ in $[Tb_2(tmh)_6dpbp]$ (Figure S6) provides inefficient back-energy transfer, resulting in relatively high Φ_{tot}.

Table 2. Photophysical properties of $[Eu_2(tmh)_6dpbp]$, $[Tb_2(tmh)_6dpbp]$, and $[EuTb(tmh)_6dpbp]$.

complex	τ_{obs}[a] [ms]	Φ_{ff}[b] [%]	Φ_{tot}[c] [%]	k_r[d] [10^3 s^{-1}]	k_{nr}[e] [10^2 s^{-1}]
$[Eu_2(tmh)_6dpbp]$	0.62	66±3	0.5±0.1	1.1	5.2
$[Tb_2(tmh)_6dpbp]$	0.96	>61±1	56±2	>0.6	<4.6
$[EuTb(tmh)_6dpbp]$	0.76 ($^5D_0 \rightarrow ^7F_2$)	—	—	—	—
$[EuTb(tmh)_6dpbp]$	0.90 ($^5D_4 \rightarrow ^7F_5$)	—	—	—	—

[a] Emission lifetime was measured excited at 355 nm (Nd:YAG laser, third harmonics). [b] Emission quantum yield of 4*f*-4*f* transition for Eu^{III} and Tb^{III} was measured with an integrating-sphere unit excited at 464 nm ($^5D_2 \leftarrow ^7F_0$) and 483 nm ($^5D_4 \leftarrow ^7F_6$), respectively. [c] Total emission quantum yield was also measured using an integrating-sphere unit excited at 330 nm. [d] Radiative rate constant was estimated from $k_r = \Phi_{ff} / \tau_{obs}$. [e] Non-radiative rate constant was calculated from $k_{nr} = (1/\tau_{obs})-k_r$.

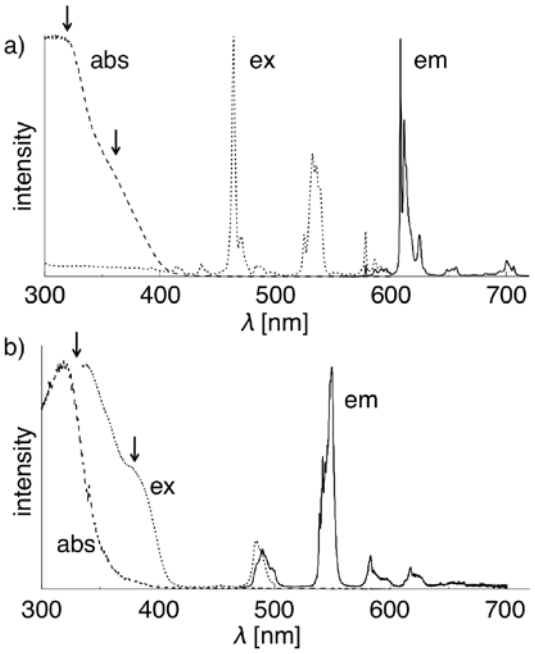

Figure 3. Diffuse reflection (broken line), excitation (dotted line), and emission (solid line) spectra of a) $[Eu_2(tmh)_6dpbp]$ and b) $[Tb_2(tmh)_6dpbp]$ in the solid state at room temperature.

Figure 4. a) Emission spectra of $[EuTb(tmh)_6dpbp]$ at 100-400 K. b) The ratio of emission spectral area of $^5D_0\rightarrow{}^7F_2$ (A_{Eu}) to $^5D_4\rightarrow{}^7F_5$ (A_{Tb}) at 100-450 K for $[EuTb(tmh)_6dpbp]$ (circle) and the mixture of $[Ln(tmh)_3tppo]$ (square).

Temperature-dependent luminescence

Emission spectra of $[EuTb(tmh)_6dpbp]$ in the solid state at 100-400 K are shown in Figure 4a. The luminescence intensity of $^5D_0\rightarrow{}^7F_2$ transition (611 nm) was larger than that of $^5D_4\rightarrow{}^7F_5$ transition (548 nm) at 100 K and decreased with increasing temperature. The luminescence color of $[EuTb(tmh)_6dpbp]$ gradually changed from red to green with increasing temperature (Figure 1b), being different from the luminescence behavior of previously reported Eu^{III}/Tb^{III} MOFs and coordination polymers (color change: green to red).[6,8,9,26-28] We considered that the unexpected color change is induced by the presence of a LMCT band in $[EuTb(tmh)_6dpbp]$. Temperature-dependent emission spectra of the mixture of $[Eu(tmh)_3tppo]$ and $[Tb(tmh)_3tppo]$[15] were also evaluated to confirm the effect of the dinuclear structure on the luminescent color-changing phenomenon (Figure S7). The mixture also showed red-to-green color change with increasing temperature. Figure 4b shows the ratio of the emission spectral area of $^5D_0\rightarrow{}^7F_2$ (A_{Eu}) to that of $^5D_4\rightarrow{}^7F_5$ (A_{Tb}) for $[EuTb(tmh)_6dpbp]$ and the mixture. The value of A_{Eu}/A_{Tb} for $[EuTb(tmh)_6dpbp]$ was higher than those for the mixture below 300 K. We assume that the enhanced emission at 611 nm resulted from Tb^{III}-to-Eu^{III} energy transfer through dpbp ligand.

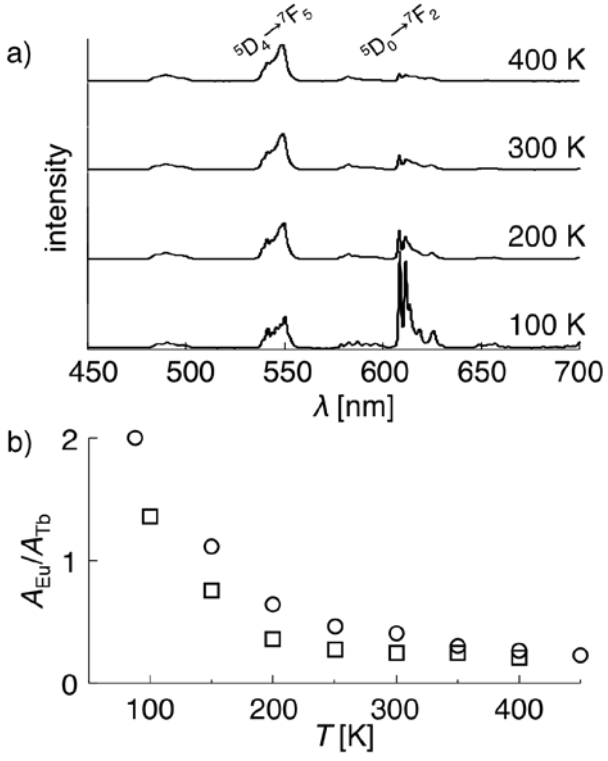

In accordance with previous reports by Brites et al., the relative thermal sensitivity (S_r) and temperature uncertainty (δT) were calculated.[29] The values were summarized in Table S3, and the values of S_r and δT at 88 K were 2.2 % K^{-1} and 0.01 K, respectively. The sensor reproducibility (R) was also estimated from 10 consecutive measurements for the ratio of luminescence integrated intensities (Figure S8), and the value of R was found to be 99.4%.

An energy diagram for energy transfer processes of $[EuTb(tmh)_6dpbp]$ are proposed in Figure 5. Under irradiation, the tmh ligand is excited to a singlet state, S_1 (30,300 cm^{-1}), and undergoes intersystem crossing to T_1 (25,600 cm^{-1}) owing to the large spin-orbit interaction of the Tb^{III}-tmh unit. The triplet state of tmh ligands (T_{tmh}) generates excited $^5D_4$ of Tb^{III} by photosensitized energy transfer, which is obviously shown by the excitation spectrum. Energy transfer from S_1 to $^5D_4$ also occurs although the rate constant is generally smaller than that from T_1 to $^5D_4$.[30] Energy transfer from S_1 and T_1 of tmh ligand to Eu^{III} is not efficient because of the presence of LMCT state that is main deactivation process. According to previous reports for temperature-dependent luminescence of the 'chameleon luminophore', the combination of Tb^{III} with dpbp induces energy transfer from $^5D_4$ to the triplet state of dpbp (T_{dpbp}).[9,11] The energy level of T_{dpbp} (22,100 cm^{-1}) was higher than the emitting levels of Tb^{III} ($^5D_4$: 20,500 cm^{-1}) and Eu^{III} ($^5D_0$: 17,300 cm^{-1}). This energy balance with activation energy provides temperature-dependent energy transfer from Tb^{III} to Eu^{III}. Excitation spectrum of $[EuTb(tmh)_6dpbp]$ monitored at 611 nm ($^5D_0\rightarrow{}^7F_2$) shows photosensitized band in the UV region (Figure S9). In addition, an emission spectrum of $[EuTb(tmh)_6dpbp]$ excited at 484 nm ($^5D_4\leftarrow{}^7F_6$) exhibited emission band based on $^5D_0\rightarrow{}^7F_2$ transition of Eu^{III} (Figure S10).

According to the previous reports, energy transfer through dpbp promotes effective emission from Eu^{III}.[9,31] In the Eu^{III}/Tb^{III} mixed complexes, the energy transfer efficiency increased with increasing temperature, resulting in gradual color change from green to red (Figure S11). The temperature-dependent energy transfer rate constants (k_{EnT}) of $[EuTb(tmh)_6dpbp]$ were also calculated using emission lifetimes of $[Tb_2(tmh)_6dpbp]$ and $[EuTb(tmh)_6dpbp]$ (Figure S12a).[32] Recently, Rodrigues and co-workers calculated rate constants of energy transfer ($^5D_4\rightarrow{}^5D_0$ and $^5D_4\rightarrow{}^5D_1$) using multipolar and exchange mechanism.[33] In our system, the relatively long distance between lanthanide ions in the crystal structure (the minimum is 10.2 Å) indicates that the contribution of exchange mechanism is not much effective. Calculated value of k_{EnT} increased with increasing temperature above 350 K. The Arrhenius plot of k_{EnT} indicated that $[EuTb(tmh)_6dpbp]$ presented temperature-dependent energy transfer with activation energy (Figure S12b). The Arrhenius analysis also suggests that the activation energy (3,700 cm^{-1}) is attributed to back energy transfer from $^5D_4$ to T_{dpbp} rather than that to T_{tmh}. In this study, unexpected red-to-green luminescence color change of $[EuTb(tmh)_6dpbp]$ was observed despite the

temperature-dependent energy transfer from Tb^{III} to Eu^{III}. We consider that the color change is caused by the state transitions from $^5D_0$ to LMCT.

A state transition from $^5D_0$ to LMCT has been found in previous studies.[12,14] The emission lifetime of $[Eu_2(tmh)_6dpbp]$ at 100-400 K was measured for investigation of the state transition (Figure S13). The values of τ_{obs} in the range of 100-300 K were approximately constant and decreased with increasing temperature above 300 K. The temperature-dependent τ_{obs} for $[Eu_2(tmh)_6dpbp]$ is similar to those for Eu^{III}-tmh complexes in our previous study.[14] The decrease in τ_{obs} is based on the state transition from $^5D_0$ to LMCT because the activation energy (2,900 cm^{-1}) is smaller than the energy gap between $^5D_0$ and T_{dpbp}. We consider that the unexpected color change of $[EuTb(tmh)_6dpbp]$ is caused by the state transition process. The quenching process related to the LMCT state in $[EuTb(tmh)_6dpbp]$ provide unexpected thermosensitive luminescence and a wide sensing range (100-450 K) compared with that in our previous study.

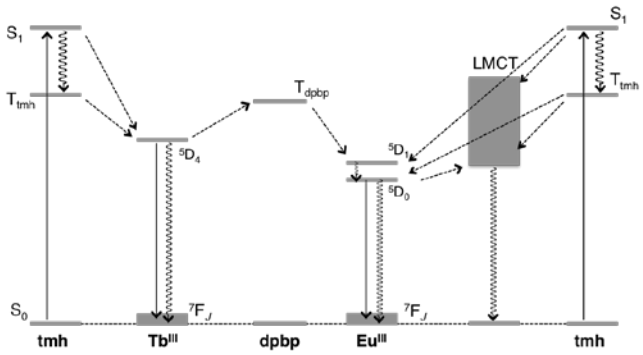

Figure 5. Energy diagram for $[EuTb(tmh)_6dpbp]$.

Conclusions

We successfully synthesized a dinuclear Eu^{III}/Tb^{III} complex with a seven-coordinate structure by means of binding two units of lanthanide-tetramethylheptanedionate through a bidentate phosphine oxide linker ligand. The observed luminescence color change (red to green) with increasing temperature is based on the presence of a LMCT state in combination with Eu^{III} and tmh ligands. The LMCT state induces the state transition from $^5D_0$ to LMCT. The presence of a LMCT band in the lanthanide luminophore is effective for thermosensing measurements in a wide range. This study provides significant thermosensing ability and new aspects for an energy transfer process in the field of luminescent lanthanide complexes.

Experimental Section

Materials: Europium chloride hexahydrate (99.9%), terbium chloride pentahydrate (99.9%), and gadolinium chloride hexahydrate (99.9%), ammonia aqueous solution (28%) and H_2O_2 aqueous solution (30%) were purchased from Wako Pure Chemical Industries Ltd. Chlorodiphenylphosphine (PPh_2Cl), 2,2,6,6-tetramethylheptane-3,5-dion, *n*-BuLi (in *n*-hexane, 1.6 M), and 4,4'-dibromobiphenyl were obtained from Tokyo Kasei Organic Chemicals. All other chemicals and solvents were reagent-grade and were used without further purification.

Apparatus: Elemental analyses were performed with an Exeter Analytical CE440. IR spectra were recorded using a JASCO FT/IR-4600 spectrometer. ^1H NMR (400MHz) spectra were measured by JEOL ECS400. Chemical shifts were reported in δ ppm, which is referenced to an internal tetramethylsilane (TMS) standard. Mass-spectroscopy was carried out by use of a Thermo Scientific Exactive (ESI-MS). TG-DTA measurements were performed with a Seiko Instruments Inc. EXSTAR 6000 (TG-DTA 6300) in a nitrogen atmosphere at a heating rate of 1 ºC min^{-1}.

Preparation of 4,4'-bis(diphenylphophoryl)biphenyl (dpbp):[34] 4,4'-Dibromobiphenyl (1.9 g, 6.0 mmol) was dissolved in anhydrous THF under argon and cooled to -78 ºC. A total of 2.1 equivalent of *n*-BuLi (7.9 mL, 12.6 mmol) was added dropwise. The temperature was not allowed to rise above -60 ºC during the addition. Stirring was continued for 3 h at -10 ºC, after which PPh_2Cl (2.3 mL, 12.6 mmol) was added at -78 ºC. The mixture was gradually brought room temperature, and stirred for 6 h. The mixture was quenched with 2 mL of methanol. The product was extracted with ethyl acetate, and then the extract was washed with brine for 3 times and dried over anhydrous $MgSO_4$. Volatiles were removed under reduced pressure to give an off-white solid that was filtered. The solid was dissolved in dichloromethane and cooled to 0 ºC and then 30% H_2O_2 aqueous solution (5 mL) was added to it. The reaction mixture was stirred for 2 h. The product was extracted with dichloromethane, the extracts washed with brine for three times and dried over anhydrous $MgSO_4$. Recrystallization from dichloromethane gave colorless crystals of the titled compound. Yield 1.7 g (54%), ^1H NMR (400 MHz, $CDCl_3$, 25 ºC): δ 7.67-7.80 (m, 16H), 7.45-7.60 (m, 12H) ppm.

Preparation of $[Eu_2(tmh)_6dpbp]$, $[Gd_2(tmh)_6dpbp]$, and $[Tb_2(tmh)_6dpbp]$: The precursor complexes, $[Eu(tmh)_3(MeOH)_2]$, $[Gd(tmh)_3(MeOH)_2]$, and $[Tb(tmh)_3(MeOH)_2]$, were synthesized by the same method as a previous report.[16] Europium chloride hexahydrate, gadolinium chloride hexahydrate, or terbium chloride pentahydrate (1.0 g, 2.7 mmol) was dissolved in distilled water (5 mL) in a 100 mL flask. An ethanol solution (20 mL) of tmh (1.46 g, 8.1 mmol) was added to the aqueous solution. An ammonia solution was added dropwise to the flask until pH 7. After stirring at room temperature for 6 h, the reaction mixture was poured into cold water (300 mL) in a conical flask. The produced precipitate, $[Eu_2(tmh)_6]$, $[Gd_2(tmh)_6]$, or $[Tb_2(tmh)_6]$[12,13] was filtered, and the resulting powder was recrystallized from methanol to afford colorless block crystals of $[Eu(tmh)_3(MeOH)_2]$, $[Gd(tmh)_3(MeOH)_2]$, or $[Tb(tmh)_3(MeOH)_2]$. Each of the precursor complexes (1.0 g, 1.4 mmol) and dpbp (0.39 g, 0.7 mmol) were dissolved with methanol (30 mL) in a 100 mL flask. The solution was heated under reflux while stirring for 6 h. The reaction mixture was recrystallized in methanol to afford colorless crystals of titled compounds. $[Eu_2(tmh)_6dpbp]$: Yield 1.1 g (79%). IR (ATR) ˜v = 2,865-2,955 (m, C-H), 1,570 (s, C=O), 1,172 cm^{-1} (s, P=O). $C_{102}H_{142}Eu_2O_{14}P_2$ calcd. (%): C 62.57, H 7.31; found C 62.06, H 7.25. $[Tb_2(tmh)_6dpbp]$: Yield 1.1 g (81%). IR (ATR) ˜v = 2,865-2,955 (m, C-H), 1,572 (s, C=O), 1,173 cm^{-1} (s, P=O). $C_{102}H_{142}O_{14}P_2Tb_2$ calcd. (%): C 62.12, H 7.26; found C 61.66, H 7.21. $[Gd_2(tmh)_6dpbp]$: Yield 1.1 g (79%). IR (ATR) ˜v = 2,865-2,955 (m, C-H), 1,570 (s, C=O), 1,172 cm^{-1} (s, P=O). $C_{102}H_{142}Gd_2O_{14}P_2$ calcd. (%): C 62.23, H 7.27; found C 61.89, H 7.25.

Preparation of $[EuTb(tmh)_6dpbp]$: A Mixture of $[Eu(tmh)_3(MeOH)_2]$ (0.5 g, 0.7 mmol) and $[Tb(tmh)_3(MeOH)_2]$ (0.5 g, 0.7 mmol) was dissolved in methanol (30 mL). The dpbp ligand (0.39 g, 0.7 mmol) was added to it.

After reflux for 6 h, recrystallization from methanol provided colorless crystals of titled compound. IR (ATR) ˜v = 2,865-2,955 (m, C-H), 1,572 (s, C=O), 1,173 cm^{-1} (s, P=O). $C_{102}H_{142}EuO_{14}P_2Tb$ calcd. (%): C 62.34, H 7.28; found C 62.60, H 7.20.

Crystallography: Single crystals of lanthanide complexes were mounted on a micromesh (MiTeGen M3-L19-25L) using paraffin oil. All measurements were carried out using a RIGAKU R-AXIS RAPID imaging plate area detector with graphite monochromated Mo-K*α*. Non-hydrogen atoms were refined anisotoropically. All calculations were performed with crystal-structure crystallographic software package. The quality of CIF data was validated by the checkCIF/PLATON service. The CIF data is presented in supporting information, and the data can be also obtained from The Cambridge Crystallographic Data Centre (CCDC 1575443, 1575444, 1575445, 1584058 for [Eu_2(tmh)$_6$dpbp], [Gd_2(tmh)$_6$dpbp], [Tb_2(tmh)$_6$dpbp], and [EuTb(tmh)$_6$dpbp], respectively**)**.

Optical measurements: Emission and excitation spectra were measured with a spectrofluorometer (HORIBA Fluorolog-3). Emission quantum yields were estimated using a spectrofluorometer (JASCO FP-6300) with an integrating sphere unit (JASCO ILF-533). The wavelength dependence of the detector response and beam intensity of the Xe light source for each spectrum were calibrated using a standard light source. Emission lifetimes were measured using the third harmonic (355 nm) of a Q-switched Nd:YAG laser (Spectra-Physics, INDI-50, fwhm = 5 ns, λ = 1064 nm) and a photomultiplier (Hamamatsu Photonics, R-5108, response time < 1.1 ns). The Nd:YAG laser response was monitored with a digital oscilloscope (Sony Tektonics, TDS3052, 500 MHz) synchronized to single pulse excitation. Emission lifetimes were determined from the slopes of logarithmic plots of decay profiles. Temperature-dependent emission spectra and emission lifetimes were measured using a cryostat (Thermal Block Company SA-SB245T) and a temperature controller (Oxford Instruments ITC-502S). Diffuse reflection spectra were recorded using a spectrophotometer (JASCO V-670) with an integrating sphere unit (JASCO ISN-723).

Acknowledgements

This work was supported by a Grant-in-Aid for Scientific Research on Innovative Area of “New Polymeric Materials Based on Element-Blocks” from the Ministry of Education, Culture, Sports, Science and Technology (MEXT) (Japan; grant number 2401). K. Y. was supported by the Ministry of Education, Culture, Sports, Science and Technology through a Program for Leading Graduate Schools (Hokkaido University “Ambitious Leader’s Program”).

Keywords: Lanthanides • Luminescence • Charge transfer • Thermochemistry • Sensors

References

[1] L. H. Fischer, G. S. Harms, O. S. Wolfbeis, *Angew. Chem. Int. Ed.* **2011**, *50*, 4546–4551.

[2] J. Feng, K. Tian, D. Hu, S. Wang, S. Li, Y. Zeng, Y. Li, G. Yang, *Angew. Chem. Int. Ed.* **2011**, *50*, 8072–8076.

[3] L. Shang, F. Stockmar, N. Azadfar, G. U. Nienhaus, *Angew. Chem. Int. Ed.* **2013**, *52*, 11154–11157.

[4] G. W. Walker, V. C. Sundar, C. M. Rudzinski, A. W. Wun, M. G. Bawendi, D. G. Nocera, *Appl. Phys. Lett.* **2003**, *83*, 3555–3557.

[5] B. Dong, B. Cao, Y. He, Z. Liu, Z. Li, Z. Feng, *Adv. Mater.* **2012**, *24*, 1987–1993.

[6] C. D. S. Brites, P. P. Lima, N. J. O. Silva, A. Millán, V. S. Amaral, F. Palacio, L. D. Carlos, *Adv. Mater.* **2010**, *22*, 4499–4504.

[7] a) K. Binnemans, *Chem. Rev.* **2009**, *109*, 4283–4374. b) S. V Eliseeva, J.-C. G. Bünzli, *Chem. Soc. Rev.* **2010**, *39*, 189–227.

[8] Y. Cui, H. Xu, Y. Yue, Z. Guo, J. Yu, Z. Chen, J. Gao, Y. Yang, G. Qian, B. Chen, *J. Am. Chem. Soc.* **2012**, *134*, 3979−3982.

[9] K. Miyata, Y. Konno, T. Nakanishi, A. Kobayashi, M. Kato, K. Fushimi, Y. Hasegawa, *Angew. Chem. Int. Ed.* **2013**, *52*, 6413–6416.

[10] S. Katagiri, Y. Hasegawa, Y. Wada, S. Yanagida, *Chem. Lett.* **2004**, *33*, 1438–1439.

[11] M. Hatanaka, Y. Hirai, Y. Kitagawa, T. Nakanishi, Y. Hasegawa, K. Morokuma, *Chem. Sci.* **2017**, *8*, 423–429.

[12] M. T. Berry, P. S. May, H. Xu, *J. Phys. Chem.* **1996**, *100*, 9216–9222.

[13] Y. C. Miranda, L. L. A. L. Pereira, J. H. P. Barbosa, H. F. Brito, M. C. F. C. Felinto, O. L. Malta, W. M. Faustino, E. E. S. Teotonio, *Eur. J. Inorg. Chem.* **2015**, 3019–3027.

[14] K. Yanagisawa, Y. Kitagawa, T. Nakanishi, T. Akama, M. Kobayashi, T. Seki, K. Fushimi, H. Ito, T. Taketsugu, Y. Hasegawa, *Eur. J. Inorg. Chem.* **2017**, 3843-3848.

[15] W. M. Faustino, O. L. Malta, G. F. de Sá, *J. Chem. Phys.* **2005**, *122*, 054109.

[16] K. Yanagisawa, Y. Kitagawa, T. Nakanishi, T. Akama, M. Kobayashi, T. Seki, K. Fushimi, H. Ito, T. Taketsugu, Y. Hasegawa, *Eur. J. Inorg. Chem.* **2015**, 4769-4774.

[17] I. Baxter, S. R. Drake, M. B. Hursthouse, J. K. M. A. Malik, J. McAleese, D. J. Otway, J. C. Plakatouras, *Inorg. Chem.* **1995**, *34*, 1384–1394.

[18] J. Xu, E. Radkov, M. Ziegler, K. N. Raymond, *Inorg. Chem.* **2000**, *39*, 4156–4164.

[19] L. D. Carlos, J. A. Fernandes, R. A. Sá Ferreira, O. L. Malta, I. S. Gonçalves, P. Ribeiro-Claro, *Chem. Phys. Lett.* **2005**, *413*, 22–24.

[20] W. T. Carnall, P. R. Fields, K. Rajnak, *J. Chem. Phys.* **1968**, *49*, 4450-4455.

[21] W. T. Carnall, P. R. Fields, K. Rajnak, *J. Chem. Phys.* **1968**, *49*, 4447-4449.

[22] K. Binemans, *Coord. Chem. Rev.* **2015**, *295*, 1–45.

[23] C. Tedeschi, C. Picard, J. Aze´ma, B. Donnadieu, P. Tisnès, *New J. Chem.* **2000**, *24*, 735–737.

[24] L. Benisvy, P. Gamez, W. T. Fu, H. Kooijman, A. L. Spek, A. Meijerink, J. Reedijk, *Dalton Trans.* **2008**, 3147–3149.

[25] A. P. S. Samuel, J. Xu, K. N. Raymond, *Inorg. Chem.* **2009**, *48*, 687–698.

[26] Y. Zhou, B. Yan, F. Lei, *Chem. Commun.* **2014**, *50*, 15235–15238.

[27] Y. Wei, R. Sa, Q. Li, K. Wu, *Dalton Trans.* **2015**, *44*, 3067–3074.

[28] Q. Xu, Z. Li, Y. Wang, H. Li, *Photochem. Photobiol. Sci.* **2016**, *15*, 405–411.

[29] a) C. D. S. Brites, P. P. Lima, N. J. O. Silva, A. Millán, V. S. Amaral, F. Palacio, L. D. Carlos, *Nanoscale* **2012**, *4*, 4799–4829; b) C. D. S. Brites, A. Millán, L. D. Carlos, *Handbook on the Physics and Chemistry of Rare Earths*, *Vol. 49*, (Eds.: J.-C. G. Bünzli, V. K. Pecharsky), Elsevier Science, B. V., Amsterdam, **2016**, pp. 339–427.

[30] W. M. Faustino, L. A. Nunes, I. A. A. Terra, M. C. F. C. Felinto, H. F. Brito, O. L. Malta, *J. Lumin.* **2013**, *137*, 269–273.

[31] Y. Hirai, T. Nakanishi, K. Miyata, K. Fushimi, Y. Hasegawa, *Mater. Lett.* **2014**, *130*, 91-93.

[32] C. Piguet, J.-C. G. Bünzli, G. Bernardinelli, G. Hopfgartner, A. F. Williams, *J. Am. Chem. Soc.* **1993**, *115*, 8197-8206.

[33] C. V Rodrigues, L. L. Luz, J. D. L. Dutra, S. a Junior, O. L. Malta, C. C. Gatto, H. C. Streit, R. O. Freire, C. Wickleder, M. O. Rodrigues, *Phys. Chem. Chem. Phys.* **2014**, *16*, 14858–66.

[34] K. Miyata, T. Ohba, A. Kobayashi, M. Kato, T. Nakanishi, K. Fushimi, Y. Hasegawa, *ChemPlusChem* **2012**, *77*, 277-280.

FULL PAPER

Temperature-dependent luminescence of the dinuclear Eu^{III}/Tb^{III} complex is demonstrated. The unexpected luminescence color change from red to green with increasing temperature was observed in the dinuclear complex. The temperature-dependent luminescence properties including LMCT state are discussed.

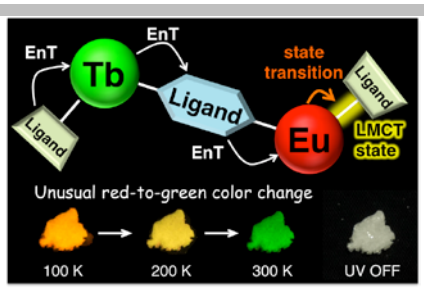

Lanthanide Luminescence

*Kei Yanagisawa, Yuichi Kitagawa, Takayuki Nakanishi, Tomohiro Seki, Koji Fushimi, Hajime Ito, Yasuchika Hasegawa**

Page No. – Page No.

A Luminescent Dinuclear Eu^{III}/Tb^{III} Complex with LMCT Band for Single-molecular Thermosensor